MOLECULAR DOCKING, DFT AND PHARMACOKINETIC STUDIES OF SOME ACETAMIDE DERIVATIVES AS POTENTIAL ANTI-BREAST CANCER AGENTS

Supported by tetfund

N. D. Magit*[1], A. B. Umar[1], K. D. Magit[2]
*[1]Department of Chemistry, Faculty of Physical Science, Ahmadu Bello University, Zaria.
[1]Department of Chemistry, Faculty of Physical Science, Ahmadu Bello University, Zaria.
[2]Department of Chemical Engineering, Faculty of Engineering, Ahmadu Bello University, Zaria.
[1]*Corresponding Author: nangnommagit@gmail.com

Received: September 14, 2023 **Accepted:** November 28, 2023

Abstract: Breast cancer is one of the extensively diagnosed cancers and the leading cause of women's cancer mortality globally. The adverse side effect and high cost of current breast cancer treatment as well as the length of time associated with the wet lab experimental methods for anti-breast cancer drug discovery makes it difficult for patients to access affordable breast cancer treatments; hence the need for Chemists to propose new potential drug candidates against breast cancer with milder side effects and whose development is less time-consuming and cost effective. Molecular docking and Density functional theory (DFT) studies, in combination with Drug-likeness and Pharmacokinetics (ADMET) predictions were utilized to examine the potency of ten (10) novel derivatives of 2-(2-methyl-1,5-diaryl-1H-pyrrol-3-yl)-2-oxo-N-(pyridin-3-yl) acetamide as potential anti-breast cancer agents with reference to the Tamoxifen Standard drug (an FDA approved drug for the treatment of breast cancer). Most of the compounds were found to have better docking scores than the control drug (Tamoxifen, Mol. Dock score = −576.584 KJ mol^{-1}). Compounds A4, A5 and A11 (with Mol. Dock scores -647.754, -663.160 and -605.082 KJ mol^{-1} respectively), which were found to be stable based of DFT studies, and whose predicted drug-likeness and pharmacokinetics properties were within the acceptable optimal requirements for drug development, emerged as the most effective compounds with better anti-breast cancer capacity than tamoxifen standard drug and are therefore proposed as potential anti-breast cancer drug candidates.

Keywords: Density Functional Theory (DFT), Drug-likeness, Molecular Docking, Pharmacokinetics

Introduction

Cancer according to the National Cancer Institute (NCI), is a disease in which some cells of the human body grow uncontrollably and spread to other parts of the body. Cancer has been identified as one of the leading causes of health-related mortalities worldwide, as it accounted for nearly ten million deaths in 2020 (Lippi and Mattiuzzi, 2020). Cancer of the breast is the most common type of cancer globally and the most common type of cancer plaguing women both in developed and developing Countries such as Nigeria (Beddoe, 2019). In Nigeria for example, breast cancer constituted about 22.7% of all diagnosed cancer cases and 18.1% of all cancer-related mortalities in 2020 (Olayide et al., 2023). The current treatment options for breast cancer which include Chemotherapy, hormone therapy, targeted therapy, immuno-therapy, and radiation therapy as highlighted by the American Cancer Society (ACS), are all drug-dependent and are characterized by adverse drug side effect on patients as well as high rate of treatment failure. There is therefore need to continue the search for new drug candidates against breast cancer with higher quality and milder side effects than the existing ones. The identification and validation of lead compounds, as well as the determination of active binding sites of biological targets related to a particular lead compound in drug discovery through the wet-lab experimental methods are widely recognized for taking long time and costing a lot of money (Choudhuri et al., 2023). Consequently, the Computer Aided Drug Design (CADD) has been employed for the fast screening and design of new drug candidates. This approach which uses computational methods to model drug receptor interactions in order to evaluate if a given chemical will attach to a target and with what affinity, effectively reduces the time required to obtain valuable drugs as well as the cost implication of new drug discovery (Choudhuri et al., 2023). Molecular docking, which is an excellent computational technique used for filtering series of chemical libraries to identify potential chemicals that could be used to find the binding capacity for a specific target, is widely used to select the best alignment of drug candidates in the active site of a protein and predict their affinity (Umar and Uzairu, 2023). Other authors have also extensively used molecular docking simulation to investigate the biological activity of various chemical structures (Umar and Uzairu, 2023; Umar et al., 2023). Density Functional Theory (DFT) which is a quantum-mechanical (QM) method used in chemistry and physics to calculate the electronic structure of atoms, molecules and solids is widely regarded as the most comprehensive technique with lower computational cost compared to many other computational approaches (Umar et al., 2023). In fact, DFT computations currently produces the most accurate and reliable result for a variety of chemical systems that are well matched with experiments (Umar et al., 2023). Other virtual screening methods for the approval of compounds that may exhibit physiological activity, drug-likeness and pharmacokinetic properties are based on a combination of experimental findings reported in various drug databases (Umar and Uzairu, 2023).

In this research, ten (10) derivatives of 2-(2-methyl-1,5-diaryl-1H-pyrrol-3-yl)-2-oxo-N-(pyridine-3-yl) acetamide synthesized and added to the chemical library by (Moghadam et al., 2020) were computationally investigated by using the molecular docking simulation, DFT calculations as well as the pharmacokinetic predictions to evaluate their anti-breast cancer activity and predict the lead compound(s) with potent pharmacological properties as a

potential drug(s) against breast cancer with reference to the tamoxifen standard drug.

Materials and Methods

Ligand Selection and Sketching

Ten (10) novel acetamide derivatives as well as the tamoxifen standard drug were retrieved from the literature (Moghadam et al., 2020). Two-dimensional (2D) structure of the compounds and the standard drug was drawn using the Chem-Draw software (version 12.0.2).

Ligand Preparation and Geometric Optimization

The sketched 2D structures of all the compounds were imported to the Spartan 14 software interface, which enabled their transformation into 3D format. Energy minimization of the compounds (in their 3D format) was done using the MM2 force field in the spartan 14 to help the docking program detect the bioactive conformer from the local minima. Geometric optimization of the compounds was done using the Density Functional Theory (DFT) method at the B3LYP level of theory and 6-311+G* basis set in order to find the most stable conformer(s) of all the compounds. The results were then saved in a separate folder in PDB file format ready for docking.

Receptor (Protein) preparation and Molecular docking

The crystal structure of the Human Estrogen Receptor ligand-binding Domain (PDB ID: 1ERR) co-crystallized with tamoxifen was downloaded from the Protein Databank at (https://www.rcsb.org/) and prepared using the Molegro Virtual Docker version 6.0 (MVD) software by eliminating water molecules, co-factors and the tamoxifen found in the complex structure. The potential ligand-binding cavity of the human estrogen receptor was predicted, and the binding cavity was set inside a restricted sphere of X:54:59, Y: 37:54, Z: 69:96 with a radius 33 Å having a grid resolution of 0.30 Å. For the molecular docking, all the prepared compounds (ligands), including tamoxifen (reference-inhibitor), were imported into the Molegro Virtual Docker 6 while Discovery Studio (DS) Visualizer was adopted to visualize various intermolecular interactions.

Drug-likeness and Pharmacokinetic (ADMET) Properties Investigation

Selected compounds from the molecular docking analysis as well as the tamoxifen standard drug were assessed for their drug-like behavior through the SwissADME (https://www.swissadme.ch/) online server while the analysis of the pharmacokinetic parameters required for Absorption, Distribution, Metabolism, Excretion and Toxicity (ADMET) was performed using the pkCSM (https://www.biosig.lab.uq.edu.au/pkCSM) online server.

Density Functional Theory (DFT) Calculations

The electronic and structural properties of the five best hit compounds selected from the docking investigation were calculated using the DFT method at the B3LYP level of theory and 6– 311G* basis set aided by Spartan 14 software. The calculated parameters used in this study include the highest occupied molecular orbital (HOMO) energies, the lowest unoccupied molecular orbital (LUMO) energies and energy gap (ΔE). Other reactivity parameters calculated using the relevant equations (equations 1-6) include; chemical-hardness(η), softness(σ), electronegativity(χ) chemical-potential(μ) and electrophilicity-index (ω). The molecular electrostatic potential surfaces (MEPs) were obtained from the population analysis calculations and visualized using Spartan 14 software.

$$\Delta E = E_{LUMO} - E_{HOMO} \quad (1)$$

$$\eta = -\frac{1}{2}(E_{HOMO} - E_{LUMO}) \quad (2)$$

$$\sigma = \frac{1}{n} = -\left(\frac{2}{E_{HOMO} - E_{LUMO}}\right) \quad (3)$$

$$X = \frac{-(E-HOMO+E-LUMO)}{2} \quad (4)$$

$$\mu = -X \quad (5)$$

$$\omega = \frac{X^2}{2\eta} \quad (6)$$

Results and Discussion

Molecular Docking Studies

The molecular docking simulation studies of the ten (10) novel acetamide derivatives (Table 1) and the tamoxifen standard drug in the active site of the Human Estrogen Receptor Ligand-binding Domain (PDB ID: 1ERR), showed that most of the studied compounds (ligands) docked at the active site of the enzyme with favorable docking and re-rank scores compared to the Tamoxifen native ligand. The docking results for the top five hit ligands from the acetamide derivatives (A4, A5, A6, A8 and A11) and their interactions with the human estrogen receptor are presented in Table 2, and were further investigated to explore the performance of the outstanding docking scores. The Discovery Studio Visualizer was used to visualize and identify key contributing residues in the binding pocket of the Human estrogen receptor of the five selected complexes (Table 2).

Table 1: IUPAC Nomenclature and Structures of the Acetamide Derivatives Studied

S/N	IUPAC Nomenclature of Compounds	Structure of Compounds
A1.	2-(5-(4-chlorophenyl)-2-methyl-1-phenyl-1H-pyrrol3-yl)-2-oxo-N-(pyridin-3-yl) acetamide	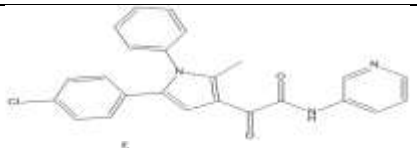
A2.	2-(5-(4-chlorophenyl)-1-(4-fluorophenyl)-2-methyl1H-pyrrol-3-yl)-2-oxo-N-(pyridin-3-yl) acetamide	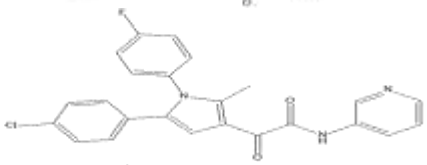
A4.	2-(5-(4-chlorophenyl)-2-methyl-1-(p-tolyl)-1Hpyrrol-3-yl)-2-oxo-N-(pyridin-3- yl) acetamide	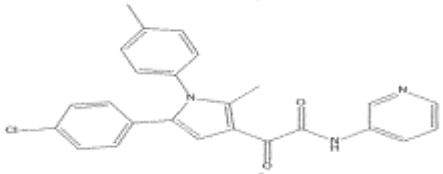
A5.	2-(5-(4-chlorophenyl)-1-(4-methoxyphenyl)-2-methyl-1H-pyrrol-3-yl)-2-oxo-N-(pyridin-3-yl) acetamide	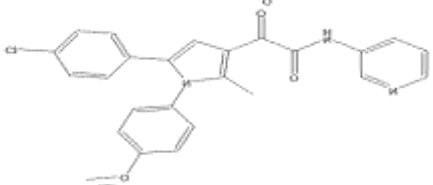
A6.	2-(2-methyl-1,5-diphenyl-1H-pyrrol-3-yl)-2-oxo-N(pyridin-3-yl) acetamide	
A7.	2-(1-(4-fluorophenyl)-2-methyl-5-phenyl-1H-pyrrol3-yl)-2-oxo-N-(pyridin-3-yl) acetamide	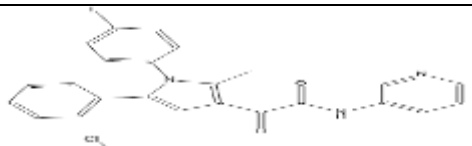
A8.	2-(1-(4-chlorophenyl)-2-methyl-5-phenyl-1Hpyrrol-3-yl)-2-oxo-N-(pyridin-3-yl) acetamide	
A9.	2-(2-methyl-5-phenyl-1-(p-tolyl)-1H-pyrrol-3-yl)-2oxo-N-(pyridin-3-yl) acetamide	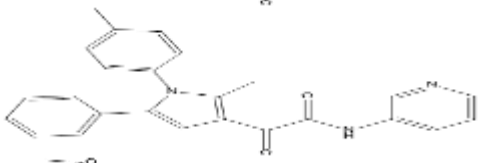
A10.	2-(1-(4-methoxyphenyl)-2-methyl-5-phenyl-1H-pyrrol-3-yl)-2-oxo-N-(pyridin-3-yl) acetamide	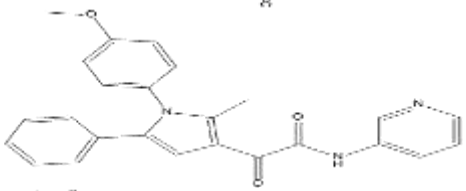
A11.	2-(2-methyl-5-phenyl-1-(3,4,5-trimethoxyphenyl)1H-pyrrol-3-yl)-2-oxo-N-(pyridin-3-yl) acetamide	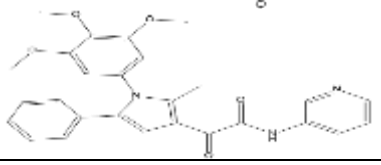

Table 2: Docking Results for the top five hit Acetamide Derivatives and their interactions with the Human Estrogen Receptor

SN	Mol. Dock Score (KJ mol^{-1})	Re-rank Score (KJ mol^{-1})	Hydrogen Bond (HB)	Bond Length (Å) for HB	C-H Bond	Alkyl	Pi-Alkyl	Others
A5.	-663.160	-495.135			HIS377 TYR459 H19	MET427 MET517	TYR459 HIS513 HIS516 LEU378	ARG515 ASP374 MET427
A4.	-647.754	-488.499			HIS377 TYR459 H19	MET427 MET517	HIS377 TYR459 HIS513 HIS516 HIS516 LEU378	ASP374 MET427
A6.	-634.776	-379.911			TRP393 H18	LYS449	PHE445 ILE326 PRO324 LEU327 PRO324 ILE386	ARG394 GLU323 GLU323 GLU323 MET357
A11.	-605.082	-453.244	LEU346	2.339	ALA350 H24	ALA350 LEU387	TRP383 ALA350 LEU525 LEU525 ALA350 LEU349 ALA350 LEU387 LEU391	
A8.	-603.513	-399.426	TRP393	2.862	TRP393 H17	ILE386 LEU387 LYS449	PHE445 PRO324 ILE326 PRO324 ILE326 LEU327 PRO324 LEU320 VAL446	ARG394 GLU323 GLU323 GLU353
Tam.	-576.584	-445.709			LEU525 THR347	MET388 LEU391 LEU428	PHE404 LEU346 ALA350 LEU525 LEU384 LEU525 LEU346 LEU349 LEU387	MET343 MET421

Mol-dock score was obtained from the PLP scoring functions with a new H-bond term and extra charge schemes Re-rank score is a linear combination of E-inter (Electrostatic, Van der Waals, H-bonding, steric) between the ligand and the protein target, A4-A11: Acetamide Derivatives, Tam.: Tamoxifen standard drug.

The 3D and 2D diagrams for the interaction of the selected ligands with the receptor are also presented in figures 1 and 2 respectively.

Complex A5	
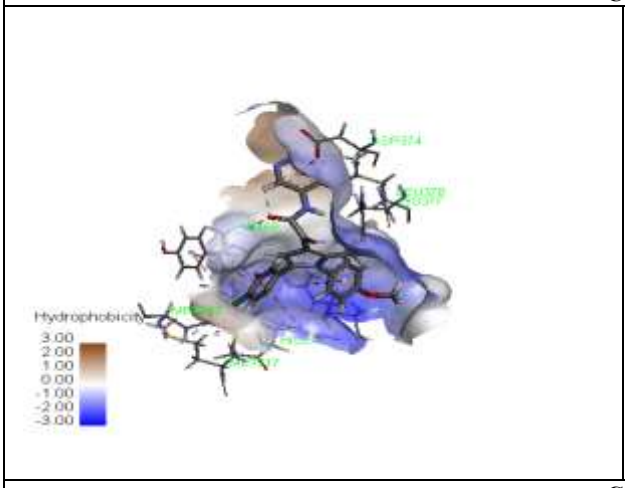	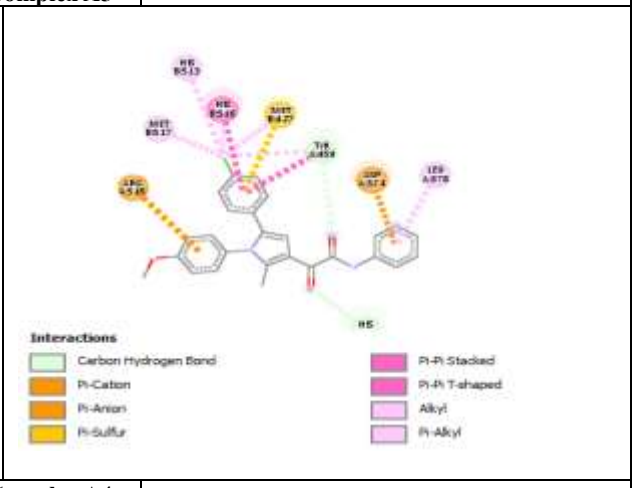
Complex A4	
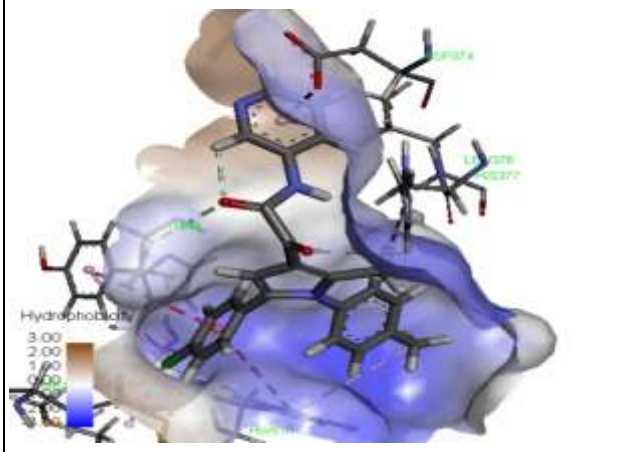	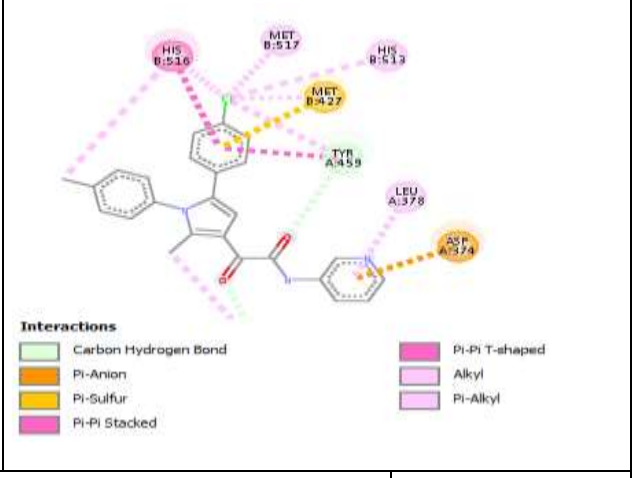
Complex A6	
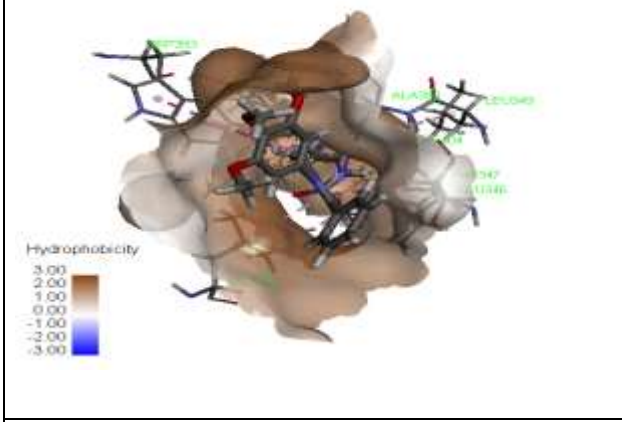	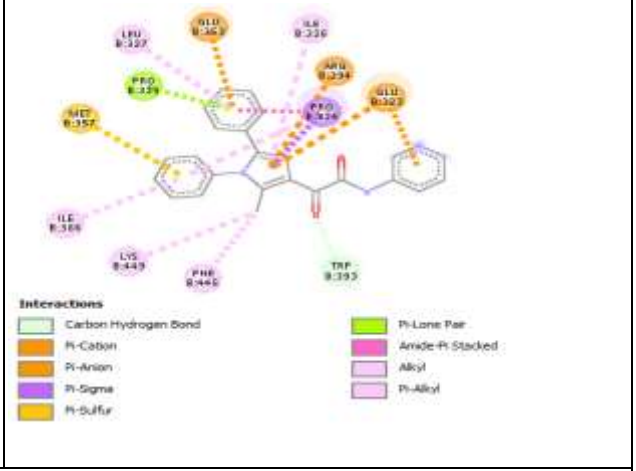

Figure 1: 3D and 2D Representations for the interactions of selected Ligands (A5, A4 and A6) with the Human Estrogen Receptor

Complex A11	

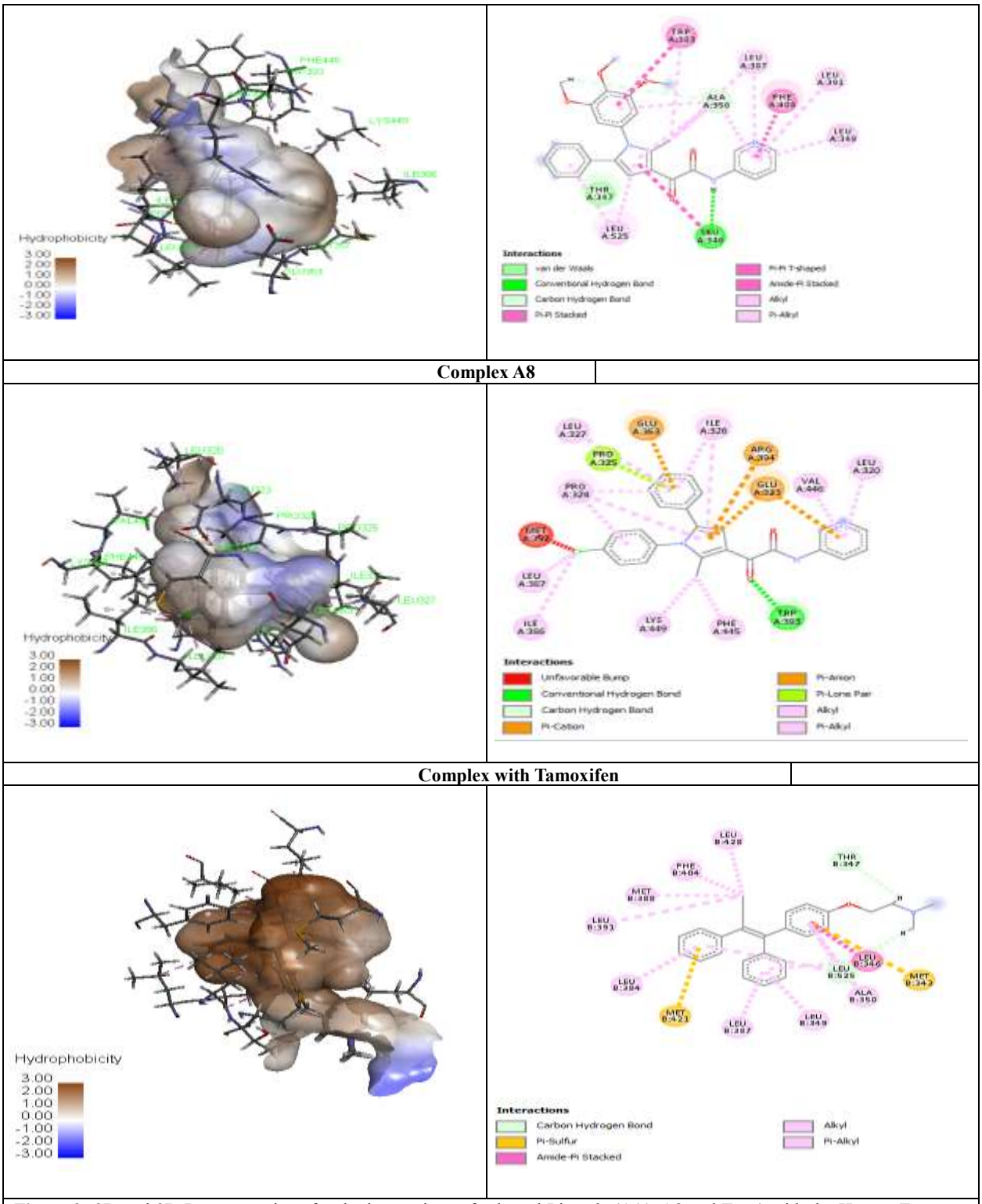

Figure 2: 3D and 2D Representations for the interactions of selected Ligands (A11, A8 and Tam.) with the Human Estrogen Receptor

From the docking results, the top five selected ligands as well as the tamoxifen native ligand formed bonds and non-bond interactions at the binding cavity of the Human estrogen receptor. The details of the complex structures with the five best docking scores as well as the tamoxifen standard drug are provided in Figures 1 and 2.

Ligand A5 in complex A5 (Figure 1) with Mol. Dock score: -663.160 KJ $mol^{-1}$and Re-rank score: -493.854 KJ mol^{-1} (Table 2) has a benzene ring which formed Pi-alkyl interactions with TYR459, HIS513, HIS516 and LEU378 residues; as well as alkyl interactions with MET427 and MET517 residues. Meanwhile, the oxygen atoms on the pyrrole moiety formed C-H bond interactions with HIS377, TYR459 and H19 residues as presented in Table 2. Furthermore, the benzene ring of this complex interacted with ARG515 and ASP374 residues via Pi-cation and Pi-anion bonds respectively. Other interactions include the Pi-Pi Stacked interaction between the quinoline moiety and TYR459 residue; as well as the Pi-Sulphur interaction between the benzene ring and MET427 residue (Table 2). Most of the interactions observed between ligand A5 and the Human estrogen receptor residues are similar to ones observed by (F Ghazi et al., 2021) in their work.

Ligand A4 in complex A4 (Figure 1) with Mol. Dock score -647.754 KJ $mol^{-1}$and Re-rank score -487.800 KJ mol^{-1} (Table 2) possess a pyrrole moiety whose oxygen atoms interacted with HIS377, TYR459 and H19 residues through C-H bond. The benzene ring of this ligand formed an alkyl interaction with MET427 and MET517 residues, as well as Pi-Alkyl interactions with HIS377, TYR459, HIS513, HIS516 (4.63338Å), HIS516 (4.98332Å) and LEU378 residues. Other interactions include; Pi-Pi Stack interaction between the benzene ring and TYR459 residue, Pi-Anion interactions between the benzene ring and ASP374 residue, and Pi-Sulphur interactions between the quinoline moiety and MET427 residue (Table 2).

In the docked complex of ligand A6 (Mol. Dock Score: -634.776 KJ mol^{-1}, Re-rank Score: -379.907 KJ mol^{-1}), as presented in Table 2 and Figure 1, the oxygen atom of the quinoline moiety formed a C-H interaction with TRP393 residue while the pyrrole moiety respectively formed an Alkyl and Pi-Alkyl interactions with LYS449 and PHE445 residues. Pi-Alkyl interactions also occurred between the benzene ring and ILE326, PRO324 (4.37127Å), PRO324 (4.63931Å), LEU327, ILE386 residues. Furthermore, Pi-Anion interactions were observed between GLU323 (4.43049Å) and the pyrrole moiety; GLU323(3.65314Å) and the quinoline moiety as well as GLU353 and benzene ring. The pyrrole moiety also exhibited a Pi-Cation interaction with ARG394 residue, while Pi-Sulphur interaction was formed between the benzene ring and MET357 residue.

Ligand A11 in complex A11 (Figure 2) inhibited Human Estrogen receptor with Mol. Dock and Re-rank Scores -605.082 and -453.244 KJ mol^{-1} respectively (Table 2). The Nitrogen atom bonded to the pyridine ring exhibited a conventional hydrogen bond interaction with LEU346 (b. l. 2.338Å), residue while C-H bond interaction exist between ALA350 residue and the pyridine moiety similar to the interactions observed by (F Ghazi et al., 2021). Akyl interactions were observed between LEU387, ALA350 residues and the pyrrole ring, with Pi-Alkyl interactions between TRP383, ALA350 (4.18397Å), LEU525 (4.30987Å), LEU525 (5.27047Å), ALA350 (5.15739Å), LEU349, ALA350 (5.05524Å), LEU387, LEU391 residues and the benzene ring, pyridine ring, pyrrole moiety, and pyridine ring respectively. Other interactions for this complex include the Pi-Stacked interaction between the benzene moiety and TRP383 residue**.**

A Mol. Dock score of -603.513 KJ mol^{-1} and Re-rank score of -399.426 KJ mol^{-1} were obtained for the docking of ligand A8 (as presented in Table 2) in the binding site of Human Estrogen Receptor (Figure 2) indicating strong interactions between the ligand and the receptor. The carbonyl oxygen atom linking the Nitrogen atom of the pyridine moiety and the pyrrole moiety interacted with TRP393 via conventional H-bond (b.l 2.338Å) (Table 2). Similar C-H interaction was also observed between the same atom and TRP393 residue of the receptor. The Cl atom attached to the benzene ring connected to the N atom of the pyridine formed a hydrophobic Akyl interaction with ILE386 and LEU387 receptor's residues, with a second alkyl interaction observed between the methyl group attached to the pyrrole ring and LYS449 residue. Furthermore, Pi-Alkyl interactions were observed between the methyl group attached to the pyrrole ring and PHE445; the benzene ring connected to the N-atom of the pyrrole moiety and PRO324 (b.l 4.78403Å) as well as the pyrrole moiety and PRO324 (b.l. 5.22132Å). Other Pi-Alkyl interactions in this complex include that between the benzene ring directly connected to the pyrrole moiety and ILE326 (b.l 4.8607Å) as well as the pyrrole moiety and ILE326 (b.l 5.07537Å); that between the benzene ring attached to the pyrrole moiety and LEU327; that between the pyridine ring and LEU320 as well as that between VAL446 and the pyridine ring. Other interactions observed in this complex (Figure 2 complex A8) are: Pi-Cation interaction between the pyrrole ring and ARG394, Pi-Anion interaction between the pyrrole ring and GLUE323 (b.l 3.79489Å) as well as that between the pyridine ring and GLUE323 (b.l 4.52255Å), and finally, Pi-Anion interaction between the benzene ring connected to the pyrrole moiety and GLU353.

As a standard comparison with the studied ligands, the native ligand (tamoxifen) was docked into the same investigated protein receptor (Human Estrogen receptor), after which a Mol. Dock score of -576.584 KJ mol^{-1} and Re-rank score of -445.709 KJ mol^{-1}(Table 2) was obtained for the standard drug, indicating that all the five selected ligands in this series have a better docking score compared to the native ligand. Visualizing the molecular interactions between the standard drug and the receptor revealed that the hydrogen atom of the methylamine group interacted with THR347 via C-H bond, while the hydrogen atom attached to the Nitrogen of the ammine group also interacted LEU525 via C-H bond. The benzene ring of the native ligand also interacted with MET343 and MET421 via Pi-Sulphur interaction. Furthermore, the methyl group attached to the ethene exhibited Alkyl interactions with LEU439, LEU428 and MET388 residues. Pi-Alkyl interactions also exist between the benzene ring and LEU343, ALA350, LEU349, LEU387, LEU384 as well as the methyl group attached to the alkene group and PHE404. The top five studied ligands were found to have superior binding affinities than the tamoxifen native ligand as seen from the docking results in table 2. The results as presented in table 2 and figures 1-2 further shows that all the top five studied acetamide derivatives (ligands) had similar protein-ligand interactions with the tamoxifen native ligand, with some of them even having better interactions than the native ligand. Since H-bonding is a significant indicator of protein-ligand solid interactions and commonly

results in high binding affinity, and the number of hydrogen bonds often increases the inhibitory potency against the target protein in protein-ligand interactions, ligands A8 and A11 with conventional hydrogen interactions (Table 2; Figure 2) showed superior protein-ligand interactions than the tamoxifen standard drug.

Drug-likeness Prediction of the top five studied Acetamide Derivatives

The SwissADME web server (https://www.swissadme.ch/) was used to perform the drug-likeness analyses of the top five studied ligands (Acetamide derivatives) as well as the tamoxifen native ligand and the result of these analyses are presented in table 3. In this section, the drug-likeness properties of the top five selected ligands (A5, A4, A6, A11 and A8) as presented in Table 3 are discussed with reference to the Lipinski's Rule of five (which states that good absorption of a molecule occurs only when: Mol. Wt. ≤500, H-bond donors ≤5, Log P ≤ 5, H-bond acceptors ≤ 10) (Lipinski et al., 2012), Verber and Muegge's rule (which states that Rotational bond ≤ 10 and topological polar surface area ≤ 140Å^2) (Veber et al., 2002) and compared with the drug-likeness properties of the tamoxifen native ligand.

Table 3: Predicted Drug-likeness Properties of the top five studied Acetamide Derivatives (Ligands) and Tamoxifen Standard drug

SN	Mol. Wt.	HBA	HBD	Log P	TPSA(Å^2)	NRB	BA
A4.	**429.90**	**3**	**1**	**5.63**	**63.99**	**6**	**0.55**
A5.	**445.90**	**4**	**1**	**5.33**	**73.22**	**7**	**0.55**
A6.	**381.43**	**3**	**1**	**4.67**	**63.99**	**6**	**0.55**
A8.	**415.87**	**3**	**1**	**5.32**	**63.99**	**6**	**0.55**
A11.	**471.50**	**6**	**1**	**4.70**	**91.68**	**9**	**0.55**
Tam.	**371.50**	**2**	**0**	**5.77**	**12.47**	**8**	**0.55**

Mol. Wt.: molecular weight; HBA: hydrogen bond acceptor; HDB: hydrogen bond donor; NRB: number of rotatable bonds; TPSA: topological polar surface area, BA: Bioavailability Score; A4-A11: Acetamide derivatives; Tam.: Tamoxifen native ligand

It can be seen from table 3. that the Molecular weights of the top five selected ligands (A4, A5, A6, A11 and A8) are in the range 381.43 to 471.50 gmol^{-1} with ligand A11 having the highest value of 471.50 gmol^{-1} indicating the compliance of the compounds to the Lipinski's molecular weight rule. The results also showed that all the top five compounds have H-bond donors and H-bond acceptors less than 5 and less than 10 respectively, with compound A11 having the highest number of H-bond acceptors as 6. Furthermore, the results as presented in table 3 shows that all the top five ligands with the exception of ligand A4 have Log P values approximately ≤5 indicating that only ligand A4 with Log P = 5.63 violates one of the Lipinki's rule of five. Generally, however, all the top five ligands in this series obey the Lipinki's rule.

The result of this study further shows that the top five best ligands all have rotatable bonds (NRB) ≤ 10 with ligand A11 having the highest NRB of 9, and topological polar surface area (TPSA) ≤ 140Å^2 with same ligand (A11) having the highest TPSA value of 91.68 Å^2. This shows that all the top five studied acetamide derivatives (ligands) obey the Verber and Muegge's rule and are said to have good drug-likeness properties, similar to the tamoxifen native ligand which also perfectly obeyed the three rules.

Pharmacokinetics (ADMET) Properties Prediction of the top five studied Acetamide Derivatives

The pkCSM online web server (https://www.biosig.unimelb.edu.au/pkCSM/) was used to perform the pharmacokinetics predictions of the top five studied acetamide derivatives (ligands) in order to confirm the Absorption, Distribution, Metabolism, Excretion and Toxicity (ADMET) properties of these compounds in the human body as potential drugs. The result of the pharmacokinetic properties of these acetamide derivatives as well as the tamoxifen native ligand is presented in Table 4.

Table 4: Predicted ADMET Properties for the top five studied Acetamide Derivatives(ligands) and Tamoxifen Standard drug

	Absorption	**Distribution**			**Metabolism**					**Excretion**			**Toxicity**
					Substrate		**Inhibitor**						
					CYP								
SN	**Intestinal Absorption**	**VDss (human)**	**BBB permeability**	**CNS Permeability**	**2D6**	**3A4**	**1A2**	**2C19**	**2C9**	**2D6**	**3A4**	**Total clearance**	**AMES toxicity**
	Numeric (%absorbed)	**Numeric (log L kg^{-1})**	**Numeric (log BB)**	**Numeric (log PS)**				**(yes/no)**				**Numeric (log mL min^{-1} kg^{-1})**	**(yes/no)**
A4.	94.943	0.395	0.132	-1.743	No	Yes	Yes	Yes	Yes	No	Yes	-0.072	No
A5.	96.774	0.447	-0.823	-2.058	No	Yes	No	Ye	Yes	No	Yes	0.015	No
A6.	95.852	0.205	0.183	-1.946	No	Yes	Yes	Yes	Yes	No	Yes	0.279	Yes
A8.	94.762	0.311	0.151	-1.825	No	Yes	Yes	Yes	Yes	No	Yes	-0.016	Yes
A11.	98.955	0.179	-1.059	-3.509	No	Yes	No	Yes	Yes	No	Yes	0.419	No
Tam.	98.612	0.621	1.327	-1.412	No	Yes	Yes	Yes	No	Yes	Yes	0.572	Yes

VDss: volume of distribution; BBB: blood-brain barrier; CNS: central nervous system; CYP: Cytochrome P

The top five studied acetamide derivatives (ligands) have intestinal absorption ranging from 94.762 (ligand A8) to 98.955% (ligand A11) as presented in Table 4. while the tamoxifen native ligand has a value of 98.612%. This shows that the five studied compounds can easily be absorbed into the human intestine with ligand A11 even having a better intestinal absorption than the native ligand. volume of distribution at steady state (VDss) which is the apparent volume of distribution after enough time has passed for the drug to distribute uniformly through all tissues, has standard accepted values in the range -0.5 to 0.5. A high VDss value (>0.5) indicates that the drug is well distributed in the plasma, while a low VDss value (<-0.5) indicates that the drug has a poor ability to cross the cell membrane (Umar et al., 2020). The predicted VDss values for the top five studied ligands as presented in Table 4. ranges between 0.179 (ligand A11) and 0.447 L kg^{-1} (ligand A5) while that of the native ligand (SD) is 0.621 L kg^{-1}. This shows that the top five studied ligands in this series have a reasonable plasma distribution within the acceptable range.

The Blood-Brain Barrier (BBB) permeability and Central Nervous System (CNS) permeability which are also important factors in achieving optimum pharmacology in drugs are measured as log BB and log PS respectively. For a given Compound, a log BB value > 0.3 implies that the compound can readily cross the BBB, while a log BB value < -1 implies that the molecule is poorly distributed to the brain. Similarly, a log PS value > -2 for a compound implies that the compound can readily penetrate the CNS while a log PS value < -3 for a compound indicates that the compound is unable to penetrate the CNS (Pires et al., 2015). The log BB values of the top five studied ligands in this series which ranges between -1.059 (ligand A11) and 0.183 (ligand A6) as presented in Table 4. shows that the selected compounds have optimum distribution to the brain. In the same vein, the log PS values of the studied ligands as presented in Table 4 ranges between -3.509 (ligand A11) and -1.743 (ligand A4) which also implies that the studied compounds have good penetration of the CNS. Cytochrome P450 which is a vital metabolizing enzyme in the human body has five major isoforms: CYP1A2, CYP2C19, CYP2C9, CYP2D6 and CYP3A4 (Umar et al., 2020). The results of the five studied ligands in Table 3 reveals positive inhibition capability for these enzymes by the studied ligands; and implies that they are safe in Pharmacokinetics interactions. Total clearance which is related to bioavailability is important for determining dosing rates to achieve steady-state concentrations is measured in log mL min^{-1} kg^{-1} (Pires et al., 2015). The faster the molecule's excretion, the higher the total clearance value and vice versa. All the selected ligands therefore, demonstrated good acceptability in the body. AMES toxicity is used to determine whether or not a drug candidate is toxic. The results in Table 4 shows that out of the top five acetamide derivatives (ligands) studied, ligands A4, A5 and A11 are non- toxic in the human body.

DFT calculations of the top five studied Acetamide Derivatives (ligands)

The frontier Molecular Orbital energies (E_{HOMO} and E_{LUMO}) and the global reactivity parameters of the top five studied ligands are presented in Table 5.

Table 5: Frontier Molecular Energies and Calculated Global Reactivity Parameters of the Ligands

SN	E-HOMO (eV)	E-LUMO (eV)	ΔE (eV)	η (eV)	σ (eV^{-1})	□ (eV)	μ (eV)	ω (eV)
A4.	-5.94	-2.20	3.740	1.870	0.535	4.070	-4.070	4.429
A5.	-5.94	-2.17	3.770	1.885	0.531	4.055	-4.055	4.362
A6.	-5.86	-2.14	3.720	1.860	0.538	4.000	-4.000	4.301
A8.	-5.99	-2.24	3.750	1.875	0.533	4.115	-4.115	4.516
A11.	-5.84	-2.11	3.730	1.865	0.536	3.975	-3.975	4.236

The energy of highest occupied molecular orbital (E-HOMO), energy of lowest unoccupied molecular orbital (ELUMO) Energy bandgap (ΔE), chemical hardness (η), chemical softness (σ), global electronegativity (□), chemical potential (μ), electrophilicity (ω)

A high HOMO value for a molecule denotes that the molecule is a good electron donor, whereas a low HOMO value indicates that the molecule is a weak electron acceptor (Manoj et al., 2022). Furthermore, a smaller energy gap (ΔE) between the LUMO and HOMO energies has a significant influence on intermolecular charge transfer and molecule bioactivity. Thus, a small energy gap observed in the hit ligands positively affects the electron moving from the HOMO to the LUMO. The energy gap (ΔE) values of the top five studied ligands increases in the order: 3.720 eV (ligand A6) < 3.730 eV (ligand A11) < 3.740 eV (ligand A4) < 3.750 eV (ligand A8) < 3.770 eV (ligand A5). Thus, the reactivity order decreases accordingly as the energy gap (ΔE) increases with ligand A6 (ΔE = 3.720) being the most reactive.

Chemical hardness (η) and softness (σ) are essential descriptors for the behavior of a molecule in a chemical reaction. Hard molecules have a high resistance to changing their electronic distribution during a reaction, whereas soft molecules have a low resistance to changing their electronic distribution during a reaction. Results in table 5 for the top five studied ligands shows a high hardness value plus a low softness value. The electronegativity (χ) of a molecule measures its ability for electron attraction (Karton and Spackman, 2021). The electronegativity of the top five best ligands in this series was calculated to be in the range 3.975 (ligand A11) to 4.115 (ligand A8) indicating that the studied ligands are donor electrons. The chemical potential (μ) as presented in table 5, shows negative values for all the studied ligands, indicating good stability, and stable complex stability with the receptor. Electrophilicity (ω) which is a predictor of the electrophilic nature of a chemical specie, measures the propensity of a molecule to accept an electron, with high values of ω denoting good electrophilicity in a molecule (Umar and Uzairu, 2022). The ranking of organic molecules based on electrophilicity is as follows; molecules with ω < 0.8 eV are weak electrophiles, molecules with 0.8 eV < ω < 1.5 eV are moderate electrophiles while molecules

with ω > 1.5 eV are strong electrophiles (Umar and Uzairu, 2022). The electrophilicity values of the five selected ligands therefore shows that the compounds are strong electrophiles since their electrophilicity values ranges between 4.236 eV (ligand A11) and 4.516 eV (ligand A8).

The molecular electrostatic potential (MEP) maps of the top five investigated ligands obtained from DFT calculations are presented in Figure 3.

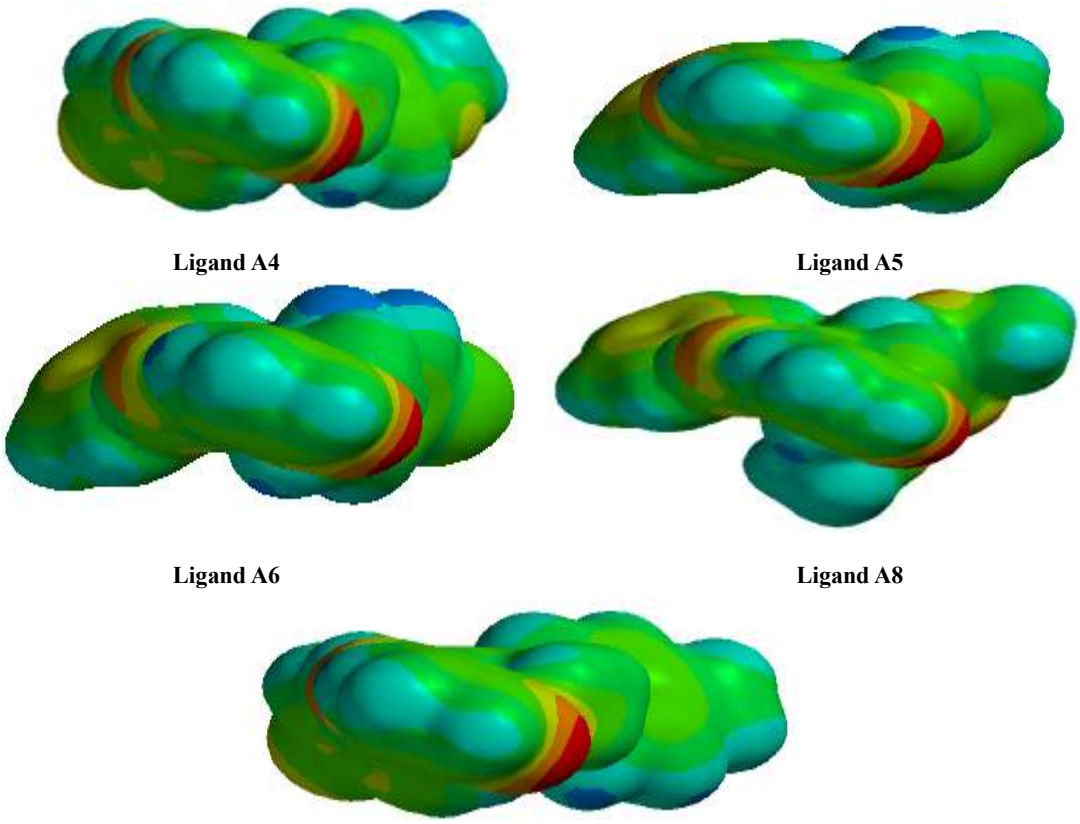

Figure 3: Molecular Electrostatic Potential (MEP) of the top five Studied Acetamide Derivatives (Ligands)

The molecular electrostatic potential (MEP) surface describes the charge distribution, which gives good insight into the physical and chemical properties of the molecule. It also predicts reactive sites for electrophilic and nucleophilic attacks in a molecule (Umar and Uzairu, 2022). From the MEP maps of the studied ligands in figure 3, red color indicates the nucleophilic region, blue indicates the electrophilic region, and the colors in-between indicate intermediate values of the MEP. Therefore, the potential increases in the order: red<orange<yellow<green<blue.

Conclusion

In this research, molecular docking simulation in combination with DFT, Drug-likeness and Pharmacokinetic studies was successfully used to virtually screen and identify potential hits against breast cancer from ten (10) novel derivatives of 2-(2-methyl-1,5-diaryl-1H-pyrrol-3-yl)-2-oxo-N-(pyridin-3-yl) acetamide. Five top-ranked compounds which exhibited superior docking scores compared to the tamoxifen native ligand (Mol. Dock score: -576.584 KJ mol^{-1}) in the active pocket of the Human Estrogen Receptor ligand-binding domain was selected by the docking studies as follows: compounds A5, A4, A6, A11 and A8 (Mol. Dock scores: -663.160, -647.754, -634.776, -605.082 and -603.513 KJ mol^{-1} respectively). The predicted drug-likeness and pharmacokinetics (ADMET) properties of these top five selected compounds revealed that three compounds consisting of compounds A4, A5 and A11 were within the acceptable optimal requirements for drug development. The DFT studies of the selected compounds using some of the global reactivity parameters such as energy gap (ΔE) chemical-hardness(η), softness(σ), electronegativity(χ), chemical-potential(μ) and electrophilicity-index (ω) further showed that the three

selected compounds (A4, A5 and A11) have energy gap values, ΔE = 3.740, 3.770 and 3.730 eV respectively, indicating their good reactivity and stability. This study therefore identified three (3) compounds (A4, A5 and A11) as potential hits with better anti-cancer activity against breast cancer than the tamoxifen standard drug.

Acknowledgement

The Authors wish to acknowledge the Department of Chemistry, Ahmadu Bello University, Zaria for its technical support during this research work. Our gratitude also goes to Dr. and Mrs. P. D. Magit for their moral and financial support towards his work.

Disclosure Statement

The Authors report no potential conflict of interest.

References

Beddoe, A. M. (2019). Elimination of cervical cancer: challenges for developing countries. ecancermedicalscience, 13.

Choudhuri, S. and Yendluri, M. and Poddar, S. and Li, A. and Mallick, K. and Mallik, S. and Ghosh, B. (2023). Recent Advancements in Computational Drug Design Algorithms through Machine Learning and Optimization. Kinases and Phosphatases, 1(2), 117-140.

F Ghazi, Y. A. and Mahdi, M. F. and Dawood, A. H. (2021). Theoretical Drug Design, Molecular Docking And ADME Study Of New 1, 3, 4-Oxadiazole Derivatives: Promising Anticancer Agents Against Both Breast And Lung Cancers. Egyptian Journal of Chemistry, 64(11), 6269-6283.

Karton, A. and Spackman, P. R. (2021). Evaluation of density functional theory for a large and diverse set of organic and inorganic equilibrium structures. Journal of Computational Chemistry, 42(22), 1590-1601.

Lipinski, C. A. and Lombardo, F. and Dominy, B. W. and Feeney, P. J. (2012). Experimental and computational approaches to estimate solubility and permeability in drug discovery and development settings. Advanced drug delivery reviews, 64, 4-17.

Lippi, G. and Mattiuzzi, C. (2020). The global burden of pancreatic cancer. Archives of Medical Science, 16(1). pp???

Manoj, K. and Elangovan, N. and Chandrasekar, S. (2022). Synthesis, XRD, hirshfeld surface analysis, ESP, HOMO-LUMO, quantum chemical modeling and anticancer activity of di (p-methyl benzyl)(dibromo)(1, 10-phenanthroline) tin (IV) complex. Inorganic Chemistry Communications, 139, 109324.

Moghadam, E. S. and Saravani, F. and Hamel, E. and Shahsavari, Z. and Alipour, M. and Hosseinkhani, S. and Ostad, S. and Amini, M. (2020). Design, Synthesis and In Vitro Anti-Cancer Evaluation of Novel Derivatives of 2-(2-Methyl-1, 5-diaryl-1H-pyrrol-3-yl)-2-oxo-N-(pyridin-3-yl) acetamide. Medicinal Chemistry, 16(3), 340-349.

Olayide, A. and Isiaka, A. and Ganiyu, R. and Samuel, O. and Halimat, A. and Olalekan, O. and Julius, O. and Anya, R. (2023). Breast Cancer Treatment and Outcomes in Nigeria: A Systematic Review and Meta-analysis. Asian Pacific Journal of Cancer Care, 8(3), 591-598.

Pires, D. E. and Blundell, T. L. and Ascher, D. B. (2015). pkCSM: predicting small-molecule pharmacokinetic and toxicity properties using graph-based signatures. Journal of medicinal chemistry, 58(9), 4066-4072.

Umar, A. B. and Uzairu, A. (2022). Exploration of Anticancer Potential of Novel Pyrrolo[2,3-b]pyridine Derivatives Targeting V600E-BRAF Kinase: Molecular Docking, Pharmacokinetic and DFT Studies. Advanced Journal of Chemistry, Section A, 5(4), 271-286. doi:10.22034/ajca.2022.356191.1322

Umar, A. B. and Uzairu, A. (2023). Molecular modeling strategy to design novel anticancer agents against UACC-62 and UACC-257 melanoma cell lines. Egyptian Journal of Basic and Applied Sciences, 10(1), 157-173.

Umar, A. B. and Uzairu, A. and Ibrahim, M. T. and Usman, A. and Habib, A. and Usman, B. (2023). Investigation of Novel Imidazole Analogues with Terminal Sulphonamides as Potential V600E-BRAF Inhibitors Through Computational Approaches. Chemistry Africa, 1-12.

Umar, A. B. and Uzairu, A. and Shallangwa, G. A. and Uba, S. (2020). Computational evaluation of potent 2-(1H-imidazol-2-yl) pyridine derivatives as potential V600E-BRAF inhibitors. Egyptian Journal of Medical Human Genetics, 21(1), 1-11.

Veber, D. F. and Johnson, S. R. and Cheng, H.-Y. and Smith, B. R. and Ward, K. W. and Kopple, K. D. (2002). Molecular properties that influence the oral bioavailability of drug candidates. Journal of medicinal chemistry, 45(12), 2615-2623.